Reprinted from JOURNAL OF ATMOSPHERIC AND OCEANIC TECHNOLOGY, Vol. 11, No. 2, April 1994
American Meteorological Society

Modeling of Downward Surface Longwave Flux Density for Global Change Applications and Comparison with Pyrgeometer Measurements

F. MISKOLCZI

Modeling of Downward Surface Longwave Flux Density for Global Change Applications and Comparison with Pyrgeometer Measurements

F. MISKOLCZI

University of Maryland, Department of Meteorology, College Park, Maryland

8 October 1992 and 28 June 1993

ABSTRACT

The success of satellite monitoring of global climate change depends on the ability to validate satellite inference methods against accurate "ground truth." Under a recent World Meteorological Organization–World Climate Research Program activity a baseline surface radiation network is being established for long-term monitoring of surface radiation balance (SRB) components. At present, it is not possible to measure all of the SRB components at known accuracies. In this paper, selected longwave surface irradiance measurements are tested against high-resolution radiative transfer computations. It is shown that the differences between the modeled IR flux density using a line-by-line code and pyrgeometer measurements are within the required accuracy for ground observations.

1. Introduction

Pyrgeometers and pyrradiometers are the standard monitoring instruments of surface downward longwave (LW) flux density and they will be used by the World Climate Research Programme (WCRP) baseline surface radiation network (BSRN) to obtain "ground truth" for validating remote-sensing methods. The BSRN accuracy requirement is 5% or 20 W m^{-2} (WCRP-54 1990). These values are consistent with a maximum of 400 W m^{-2} downward flux density typical for a wet tropical atmosphere. An absolute reference instrument has not yet been developed. It has been speculated that the range of absolute measurement errors may exceed 15% (WCRP-64 1991), which raises questions whether these instruments are adequate to meet BSRN objectives.

Several sources of measurement errors have been identified and a substantial effort has been made to improve the performance of the instruments (Albrecht and Cox 1976). The most apparent source of errors is related to the solar heating of the instrument's dome (Aldos-Arboledas et al. 1988; Enz et al. 1975; Weis 1981). By applying a shading ring, this effect can be minimized, but the shading ring may be the source of new errors. Our test measurements showed that on clear summer days an overheated metal shading ring may change the pyrgeometer reading by 20%. Degradation of the dome transmittance may easily cause 10% deviation in the instrument's response (Miskolczi and Guzzi 1993). Other sources of error are related to rapidly varying weather conditions (e.g., wind, precipitation, air temperature).

Physical model methods for estimating surface LW irradiance are based on information about temperature and humidity profiles, ozone amount, cloud cover, cloud base height, temperature, and cloud emissivity. Using the appropriate values of the above quantities and a radiative transfer model, one can compute the "true" surface LW irradiance. However, comparisons between surface irradiance measurements and computations based on simultaneous temperature and humidity soundings are rare. For clear sky conditions, radiative transfer computations implemented with soundings give a standard error of 10 W m^{-2} Schmetz (1989).

The aim of this study is to contribute to the evaluation effort of operational instruments for measuring downward LW flux density, under all sky conditions. The long-term objective is to use these instruments for monitoring LW surface flux densities at a sub-Saharan location under the influence of heavy dust, and to give an estimate on the accuracy of satellite flux retrievals based on physical or regression methods. Our initial effort focuses on situations when measuring errors due to direct solar heating of the dome are minimized.

2. Measurement of LW flux density

During 6–27 March 1992, downwelling LW surface flux density was monitored by two Eppley pyrgeometers at the National Oceanic and Atmospheric Administration (NOAA)–National Weather Service (NWS) test and evaluation facility, Sterling, Virginia, where radiosondes are launched twice a day. The instruments

Corresponding author address: Dr. Ferenc Miskolczi, Department of Meteorology, University of Maryland, College Park, MD 20742.

were mounted 1.5 m above ground and they had no shading or ventilation. The calibration of both pyrgeometers was based on the Eppley factory standards. The calibration constants were assumed to be independent on the spectral distribution of downward flux density. Parallel to the pyrgeometers, an Eppley pyranometer and a LI-COR quantum sensor were also operated. Data were acquired with a CR-10 Campbell data logger, programmed for 2-s sampling rate and 1-min integration time. Thermopile voltages were measured with 0.3-μV resolution in the 2.5-mV full-scale range. Thermistor resistances were sampled by a dc half-bridge with 3-μV resolution in the 25-mV range. The resistance–temperature conversion was performed by interpolation, using the thermistor data sheet, allowing an absolute accuracy of 0.1°C. Data reduction was based on the following equation given by Albrecht and Cox (1976):

$$L_m = aP + sT_c^4 - ks(T_d^4 - T_c^4), \qquad (1)$$

where L_m is the measured irradiance, a is the calibration constant, P is the thermopile voltage, s is the Stefan–Boltzman constant, T_d and T_c are the dome and case absolute temperatures, respectively, and k is the dome heating constant.

Simultaneous surface irradiance measurements by the two pyrgeometers are presented in Fig. 1. The bias between the two measurements is less than 0.5 W m^{-2}. The average value obtained by the two instruments was used for comparison with model computations. From the available soundings during the experiment, 41 profiles were selected as inputs for LW flux com-

TABLE 1. Input data to the LW flux model.

No.	T_s (K)	w (%)	H_2O (prcm)	C_1 ($\times 10^{-1}$)	A_1 (km)	C_2 ($\times 10^{-1}$)	A_2 (km)	C_3 ($\times 10^{-1}$)	A_3 (km)
1	280.9	97	2.61	10.0	0.14				
2	280.6	95	2.45	10.0	1.35				
3	287.6	87	2.70	3.7	1.2				
4	279.3	100	2.33	10.0	2.0				
5	288.6	70	1.93	6.0	1.7				
6	278.1	96	1.60	5.0	2.0				
7	288.8	53	1.52						
8	282.6	83	2.59	1.0	2.0	3.0	3.3	6.0	5.0
9	285.4	97	2.63	3.0	3.0	7.0	5.0		
10	275.5	95	1.00	3.0	1.0	7.0	2.2		
11	266.5	81	0.51						
12	277.1	41	0.71	1.0	2.3	1.0	8.3		
13	268.1	52	0.38						
14	273.5	34	0.38	2.5	1.1				
15	266.5	71	0.51	1.2	2.0				
16	277.1	44	0.69	2.0	2.0	2.0	3.0		
17	269.9	88	0.54	1.0	2.0				
18	273.8	33	0.43	3.0	2.0				
19	266.5	55	0.26	3.0	1.1				
20	274.9	28	0.49						
21	269.9	65	1.18	10.0	3.3				
22	285.6	44	1.83	10.0	2.3				
23	277.6	54	1.33	4.0	1.3	4.0	1.7	2.0	2.5
24	274.3	88	2.01	10.0	1.1				
25	274.3	96	2.29	10.0	0.23				
26	274.3	92	0.91	6.2	0.7				
27	271.6	96	0.71	2.0	0.7				
28	277.6	42	0.70	5.0	6.7	5.0	8.3		
29	277.0	34	0.53	4.0	2.8				
30	273.1	88	1.53	6.0	0.1				
31	275.0	39	0.51						
32	267.1	88	0.61	2.0	1.7				
33	282.0	24	0.55						
34	271.0	84	0.76						
35	284.9	33	0.89	8.0	5.0	2.0	8.3		
36	278.4	96	1.91	10.0	1.1				
37	280.4	100	1.99	10.0	0.5				
38	277.1	96	1.36	10.0	1.1				
39	270.3	96	0.82	7.5	1.35				
40	275.0	39	0.49	3.7	2.0				
41	270.3	96	1.87						

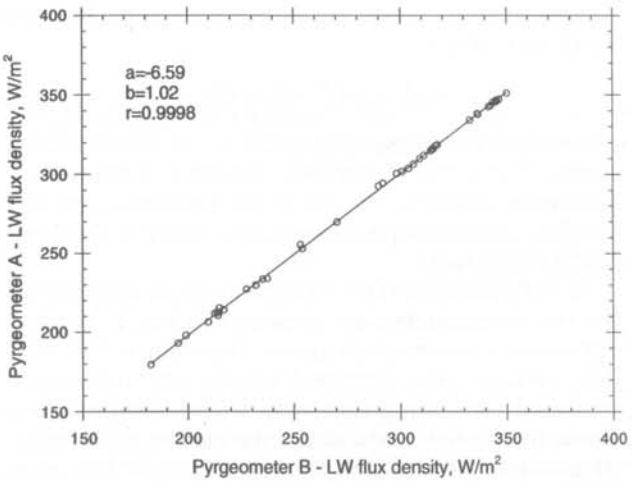

FIG. 1. Pyrgeometer comparison.

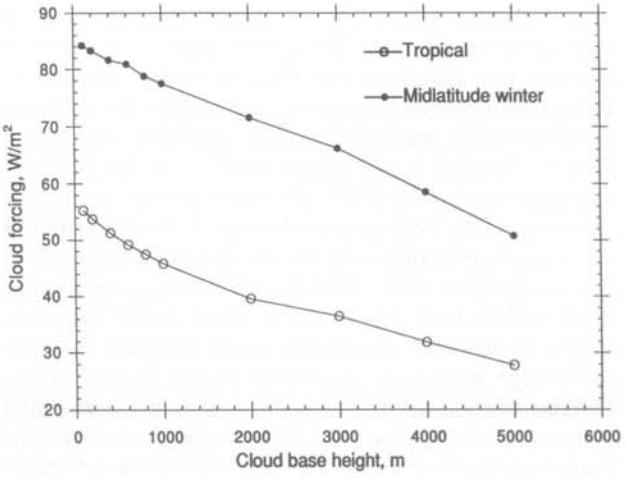

FIG. 2. Differences between the overcast and clear irradiances as the function of cloud-base height.

putations. They were generally launched around 1100 and 2300 UTC when the downward shortwave flux density did not exceed 10 W m^{-2}, reducing the dome heating due to solar radiation to a negligible level. For both pyrgeometers, a dome heating constant of $k = 4.4$ was used, giving a correction range between -7 and 5 W m^{-2}. Conventional surface observations that were used as inputs to the LW model are summarized in Table 1; T_s is the surface air temperature (K), w is the surface relative humidity (%), H_2O is the total precipitable water of a vertical (clear) air column in precipitable centimeters (prcm) computed from the radiosonde data sampled at 6 s, C_1, C_2, and C_3 are the cloud cover in tenths, and A_1, A_2, and A_3 are the cloud-base altitudes (km) for the different cloud layers. Cloud emissivity was taken as 1.0 for low- and midlevel clouds and 0.3 for high-level clouds. Daily total Dobson ozone observations from the NASA/Goddard Space Flight Center Wallops Flight Facility in Wallops Island, Virginia, were also used as inputs. In the model computations, the *U.S. Standard Atmosphere, 1976* ozone mixing-ratio profile was scaled appropriately to match with the observed total ozone amount.

TABLE 2. Differences between overcast and clear-sky flux densities (W m^{-2}) as a function of cloud base height, assuming black clouds.

Model atmosphere (Kneizys et al. 1980)	Tropical			Midlatitude winter		
Cloud-base height (km)	1	2	5	1	2	5
HARTCODE (Miskolczi et al. 1990)	45.9	39.6	27.8	78.2	72.5	51.6
ATRAD (Wiscombe et al. 1985)	49.1	42.3	29.1	77.8	71.7	50.8
Schmetz (1989)	39.0	34.0	23.0	80.0	75.0	53.0

3. Computation of the LW flux density

Line-by-line computations of LW radiation fluxes are valuable as a reference, when low-resolution computations or direct measurements have to be evaluated. In this study the surface LW irradiance was computed with the updated version of the HARTCODE radiation code as presented in Miskolczi et al. (1990). In a given spectral range the computing time is directly proportional to the number of atmospheric layers used. Therefore, it is preferred to keep the number of layers where accurate transmittance functions are computed to a minimum and to use interpolated transmittances for the radiance computations in additional layers. Us-

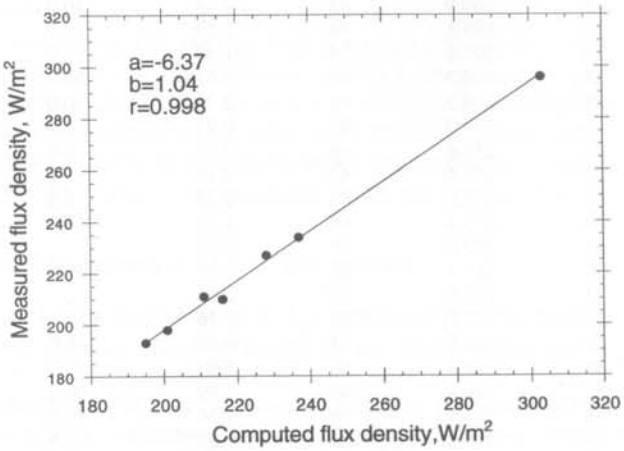

FIG. 3. Comparison of measured and computed flux densities in clear-sky cases.

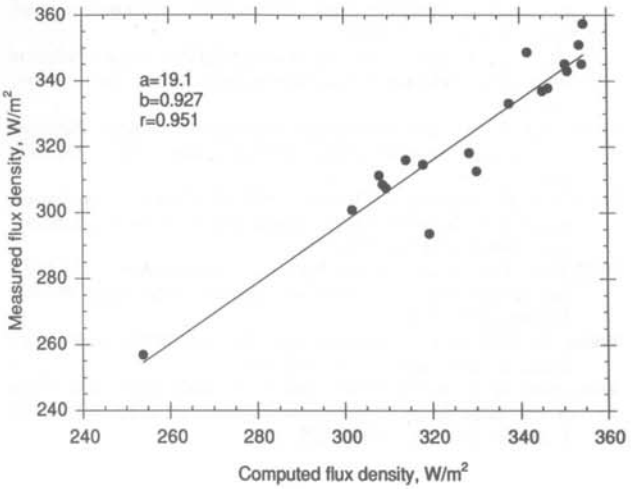

FIG. 4. Comparison of measured and computed flux densities in overcast cases.

ing HARTCODE, the spectral radiances were computed at seven zenith angles, for 160 exponentially placed layers. However, the transmittances were computed only for 16 layers, thus reducing the computing time by a factor of 10. The wavenumber integration of spectral radiances was performed numerically at each 1.0-cm^{-1} width interval between 1- and 3390-cm^{-1} wavenumbers. The total flux density was determined by the sum of the spectral flux densities. In this study only seven major absorbers (H_2O, CO_2, O_3, N_2O, CH_4, CO, and O_2) were considered. The surface irradiances were computed as follows:

$$L_c = L_o(1 - \Sigma C_i) + \Sigma C_i L_i, \qquad (2)$$

where C_i is the percentage fractional cloud cover of the ith cloud layer, and L_o and L_i are the clear and overcast flux densities. Results related to the cloud forcing by perfectly black clouds at different altitudes are presented in Table 2 and in Fig. 2. For this comparison the LOWTRAN tropical and midlatitude winter model atmospheres were used (Kneizys et al. 1980). Cloud forcing (overcast flux–clear flux) as estimated by HARTCODE and ATRAD (Wiscombe et al. 1985) is in excellent agreement, the maximum difference is 3 W m^{-2} in the tropical and 0.8 W m^{-2} in the midlatitude winter cases. Most likely, these differences are due to the different layering of the model atmospheres and, consequently, the slightly different absorber amounts.

4. Results and conclusions

The sky conditions at Sterling, Virginia, in March 1992 were mostly cloudy; there were only eight clear-sky cases during the experiment. From the remaining 33 cases, 19 were overcast and 14 were partly cloudy. Comparisons between the computed and measured fluxes are presented in Figs. 3, 4, and 5. For the clear and overcast cases the agreement between the measurements and model computations is better than for the partly cloudy ones. For clear cases, the theoretical computations agree closely with the surface irradiance measurements. The standard error is about 2.5 W m^{-2}; this is in the range of existing differences between sophisticated radiative transfer models (see Table 2). For overcast cases, the theoretical values generally overestimate the measured ones; the bias is 5.3 W m^{-2}. Based on emissivity sensitivity tests, the differences are not caused by uncertainties in cloud-base height but rather by overestimation of the midlevel cloud emissivities. In partly cloudy cases, the bias is only 0.5 W m^{-2}; the larger scatter as evident in Fig. 5 is the result of the combined effect of the errors in cloud cover and cloud emissivity. Deviations from the assumed cylindrical symmetry of the radiation field due to the inhomogeneous cloud distribution might be another source of error. For cloudy cases, identification of sources of error requires further studies with a larger database. It would seem that by using accurate radiative transfer computations we may reproduce the clear-sky pyrgeometer readings within 2–5 W m^{-2}.

Acknowledgments. This work was supported by Grant NSFD INT-9015325 to the University of Maryland. Thanks are due to the granting agency; to Dr. R. T. Pinker for help at various stages of this study; to Dr. I. Laszlo for performing the computations with the ATRAD model; to Dr. C. Daughtry for the loan of the CR-10 data logger; to R. Stone, J. McClain, and L. Winans from the NOAA/NWS test and evaluation facility at Sterling, Virginia, for valuable help with the logistic of the experiment and for providing the high-

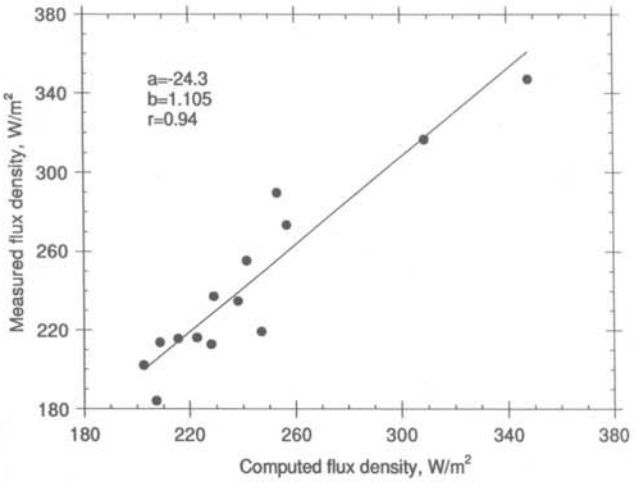

FIG. 5. Comparison of measured and computed flux densities in partly cloudy cases.

resolution soundings; and to the NASA/GSFC Wallops Island Flight Facility for providing the ozone data.

REFERENCES

Albrecht, B., and S. K. Cox, 1976: Procedures for improving pyrgeometer performance. *J. Appl. Meteor.*, **16,** 188–197.

Aldos-Arboledas, L., F. Vida, and J. I. Jimenez, 1988: Effects of solar radiation on the performance of pyrgeometers with silicon dome. *J. Atmos. Oceanic Technol.*, **5,** 666–670.

Enz, J. W., and others, 1975: Solar radiation effects on pyrgeometer performance. *J. Appl. Meteor.*, **14,** 1297–1302.

Kneizys, F. E., and others, 1980: Atmospheric transmittance/radiance: Computer code LOWTRAN5. Rep. AFGL-TR-80-67, Air Force Geophysics Laboratory, Hanscomb AFB, MA, 127 pp.

Miskolczi, F., and R. Guzzi, 1993: Effect of the non-uniform spectral dome transmittance on the accuracy of IR radiation measurements using shielded pyrradiometers and pyrgeometers. *Appl. Opt.*, **32**(18), 3257–3268.

——, R. Rizzi, R. Guzzi, and M. Bonzagni, 1990: High resolution atmospheric radiance–transmittance code. *Meteor. Environ. Sci.*, 743–790.

Schmetz, J., 1989: Towards a surface radiation climatology: Retrieval of downward irradiance from satellites. *Atmos. Res.*, **23,** 287–321.

WCRP-54, Radiation and Climate, 1991: *Workshop on Implementation of the Baseline Surface Radiation Network,* Washington, D.C., WMO-TD-No. 406, 8 pp.

WCRP-64, 1991: *Second Workshop on Implementation of the Baseline Surface Radiation Network.* Davos, Switzerland, WMO/TD-No. 453, 26 pp.

Weiss, A., 1981: On the performance of pyrgeometers with silicon dome. *J. Appl. Meteor.*, **20,** 962–965.

Wiscombe, W. J., R. M. Welch, and W. D. Hall, 1985: The effects of very large drops on cloud absorption. Part I: Parcel models. *J. Atmos. Sci.*, **41,** 1336–1355.